An analytical method for predicting surface soil moisture from rainfall observations

Feifei Pan
Environmental Sciences Division, Oak Ridge National Laboratory, Oak Ridge, Tennessee, USA

Christa D. Peters-Lidard
Hydrological Sciences Branch, NASA Goddard Space Flight Center, Greenbelt, Maryland, USA

Michael J. Sale
Environmental Sciences Division, Oak Ridge National Laboratory, Oak Ridge, Tennessee, USA

Received 10 March 2003; revised 18 June 2003; accepted 24 July 2003; published 12 November 2003.

[1] A simple analytical method for estimating surface soil moisture directly from rainfall data is proposed and studied. Soil moisture dynamics are represented by a linear stochastic partial differential equation [*Entekhabi and Rodriguez-Iturbe*, 1994]. A diagnostic equation is derived from the soil moisture dynamics equation by eliminating the diffusion term. The derived daily soil moisture function is a time-weighted average of previous cumulative rainfall over a given period (e.g., >14 days). The advantage of this method is that information on the initial condition of soil moisture, which is often not available at all times and locations, is not needed. The loss coefficient in the diagnostic equation for soil moisture can be estimated from land surface characteristics and soil properties. The method for determining the averaging window size, the loss coefficient, and the infiltration coefficient are described and demonstrated. The soil moisture data observed during three field experiments, i.e., Monsoon'90, Washita'92, and SGP'97, are compared to the calculated soil moisture. The results indicate that the proposed method is robust and has the potential for useful soil moisture predictions. *INDEX TERMS:* 1655 Global Change: Water cycles (1836); 1704 History of Geophysics: Atmospheric sciences; 1719 History of Geophysics: Hydrology; 1866 Hydrology: Soil moisture; 1854 Hydrology: Precipitation (3354); 1818 Hydrology: Evapotranspiration; *KEYWORDS:* soil moisture, precipitation, Antecedent Precipitation Index (API), loss coefficient

Citation: Pan, F., C. D. Peters-Lidard, and M. J. Sale, An analytical method for predicting surface soil moisture from rainfall observations, *Water Resour. Res.*, *39*(11), 1314, doi:10.1029/2003WR002142, 2003.

1. Introduction

[2] Soil moisture is often defined as the water content in the upper several meters of soil that is available for plant growth. It affects land surface-atmosphere interactions by influencing the partition of incoming radiation into sensible and latent heat fluxes, and the separation of precipitation into infiltration and surface runoff. Understanding of the spatial and temporal patterns of soil moisture is critical for many applications and for answering various science questions [e.g., *Hornberger et al.*, 2001; *Houser*, 1996]. The important roles of soil moisture in Earth system dynamics include: (1) atmospheric dynamics, where soil moisture can influence large-scale atmosphere circulation [*Dastoor and Krishnamurti*, 1991; *Delworth and Manabe*, 1993; *Castelli and Rodriguez-Iturbe*, 1995; *Koster et al.*, 2000; *Ducharne et al.*, 2000; *Hong and Pan*, 2000]; mesoscale dynamics [e.g., *McCumber and Pielke*, 1981; *Ookouchi et al.*, 1984; *Mahfouf et al.*, 1987; *Lynn et al.*, 1995]; and boundary layer development [e.g., *Zhang and Anthes*, 1982; *Betts et al.*,1993; *Lynn et al.*, 1995; *Quinn et al.*, 1995]; (2) water resource availability, where soil moisture is an important variable for water resource management, reservoir design and operation [*Mehrotra*, 1999], drought assessment, flood forecasting [e.g., *Viterbo and Betts*, 1999], hydrologic processes and water-balance studies; (3) agriculture, where crop production, irrigation, pest detection and control are all related to soil moisture information [e.g., *Dinar et al.*, 1986]; (4) forestry, where soil moisture is important for forest yield estimation, harvest management and forest fire prediction; (5) civil engineering, where soil moisture is useful in hazardous assessments in construction; (6) ecosystem dynamics, where soil moisture states influence biogeochemical cycles [e.g., *Weitz et al.*, 1999; *Lindberg et al.*, 1999]; and (7) soil science, where soil moisture plays an important role in erosion, mass movement, and land slides [e.g., *Govers*, 1991; *Fecan et al.*, 1999].

[3] Although soil moisture data have many applications, the observations of soil moisture are often sparse. Unlike soil moisture, precipitation is measured routinely at weather stations. Besides the routine point measurements, satellite (e.g., TRMM) and ground radar systems (e.g., NEXRAD) are utilized for measuring rainfall over large areas at long period and at high sampling frequency. Since precipitation

0043-1397/03/2003WR002142$09.00

is the primary force controlling the state and evolution of soil moisture [*Entekhabi and Rodriguez-Iturbe*, 1994], we want to develop a new, relatively simple method for estimating surface soil moisture over large areas and long periods, that can be applied with readily available atmospheric forcing data including rainfall, land cover, and soil characteristics.

[4] Several attempts have been made to link precipitation to soil moisture using Antecedent Precipitation Index (API) [e.g., *Saxton and Lenz*, 1967; *Blanchard et al.*, 1981; *Choudhury and Blanchard*, 1983; *Wetzel and Chang*, 1988; *Shaw et al.*, 1997]. However, *Saxton and Lenz* [1967] indicated that accuracy in selecting the initial API is critical for successful estimation of subsequent values. Therefore the beginning date for computing API was often chosen a few days after a heavy rain, because the initial condition of API or soil moisture is easy to define, i.e., near field capacity [*Saxton and Lenz*, 1967]. Although the effect of the initial condition decays with time, the dependence on the initial condition is a serious limitation to the API method. Finally, the API method can only be applied when soil moisture is less than field capacity [*Saxton and Lenz*, 1967].

[5] *Farago* [1985] derived a stochastic model for the estimation of soil moisture distribution based on daily rainfall and an initial value of the soil moisture. However, similar to the API method, the requirement of initial information on soil moisture condition makes Farago's method less generally applicable. *Capehart and Carlson* [1994], along with many others, have used observed precipitation and surface radiation to derive soil moisture based on soil hydrology models; however, this approach requires initial and boundary conditions, specification of radiative, thermal and hydraulic parameters, as well as significant computational resources.

[6] *Findell and Eltahir* [1997] found that the correlation of soil moisture with the moving average (with a 21-day window size) of rainfall actually is less than that of soil moisture with the subsequent precipitation. Their results imply that we could predict rainfall from soil moisture, rather than predict soil moisture from rainfall. *Entekhabi and Rodriguez-Iturbe* [1994] (hereinafter referred to as ER94) proposed a stochastic partial differential equation to represent soil moisture dynamics. This equation was utilized only to study the characteristics of the space-time variability of soil moisture in frequency and wavelength domain, rather than to derive soil moisture directly from rainfall. *Yoo et al.* [1998] used the same equation to study the impact of rainfall on soil moisture variability. Their study showed that rainfall is less important than soil texture in controlling the variability of the soil moisture field, because surface runoff, drainage, and evapotranspiration reduce the impact of rainfall and make the soil moisture field similar to soil texture field after the storm ends.

[7] A simplified diagnostic equation of soil moisture that does not depend on initial soil moisture conditions can be derived from ER94's equation. The theoretical background and derivation are presented in section 2 that follows. The justification of the proposed approximation is also given in section 2. The study areas and observed data are introduced in section 3. Methodology and results are shown in section 4. Section 5 consists of conclusions and recommendations for future development of this method.

2. Theoretical Background

[8] *Entekhabi and Rodriguez-Iturbe* [1994] assumed that the soil moisture scalar field $s(x, t)$ satisfies the following linear stochastic partial differential equation:

$$nZ\frac{\partial s}{\partial t} = -\eta s + nZ\left(\kappa\nabla^2 s\right) + I(x,t) \tag{1}$$

where x represents location, t stands for time, $s(x, t)$ is the relative saturation (i.e., the ratio of volumetric soil moisture to soil porosity), n is soil porosity, Z is the thickness of the soil layer, $-\eta s$ represents the cumulative losses of soil moisture due to evaporation or evapotranspiration and drainage, $\kappa\nabla^2 s$ is the diffusion term, and $I(x, t)$ is infiltration rate. Two coefficients are introduced in equation (1): the loss coefficient η with the dimension of [L/T], and the diffusion coefficient κ with the dimension of [L^2/T]. In equation (1) capillary rise from deeper soil layers is neglected.

[9] Similar to equation (1), the linear stochastic partial differential equation for describing the intrinsic dynamics of volumetric soil moisture $\theta(x, t)$ (with dimension [L^3/L^3]) driven by the rainfall rate $p(x, t)$ is given by:

$$Z\frac{\partial \theta}{\partial t} = -\eta\theta + Z\left(\kappa\nabla^2\theta\right) + \gamma p_{net}(x,t) \tag{2}$$

In addition to the coefficients η and κ, the infiltration coefficient γ is used to represent the ratio of infiltration rate $I(x, t)$ to net rainfall rate $p_{net}(x, t)$, which is equal to $p(x, t)$ minus interception. For nonforested regions, we may temporarily neglect the interception, and thus $p_{net}(x, t) \approx p(x, t)$.

[10] In ER94, η is assumed to be constant over both space and time, and with a magnitude of 1m/year. The lower and upper limits of the diffusion coefficient κ are 10^{-3} m^2/hr and 10^5 m^2/hr, which correspond to the diffusion taking place within the unsaturated zone and diffusion taking place by the surface runoff mechanism, respectively. The longer timescale (i.e., interstorm period, 48hr in ER94) is associated with the small diffusion coefficient (i.e., $\kappa = 10^{-3}$ m^2/hr), and the large diffusion coefficient (i.e., $\kappa = 10^5$ m^2/hr) is associated with the shorter time period (i.e., storm period, 10hr in ER94). This suggests that we may simplify the general dynamics equation by dropping the diffusion term. As *Entekhabi and Rodriguez-Iturbe* [1994] showed, diffusion is small compared to the vertical losses by evapotranspiration and percolation if the spatial redistribution of soil moisture is carried out only through groundwater flow at any timescale. At daily or longer timescales, the soil moisture field may be affected by the overland flow. Therefore, if we apply equation (2) to a timescale of one day or less, we can ignore the diffusion term. On the other hand, the upper limit of the diffusion coefficient (i.e., $\kappa = 10^5$ m^2/hr) in ER94 is estimated from the overland flow velocity. However, if the overland flow occurs on areas with relatively steep slopes, less ponded water on the surface is accumulated, and thus reinfiltration is reduced [*Dingman*, 1994]. Therefore the

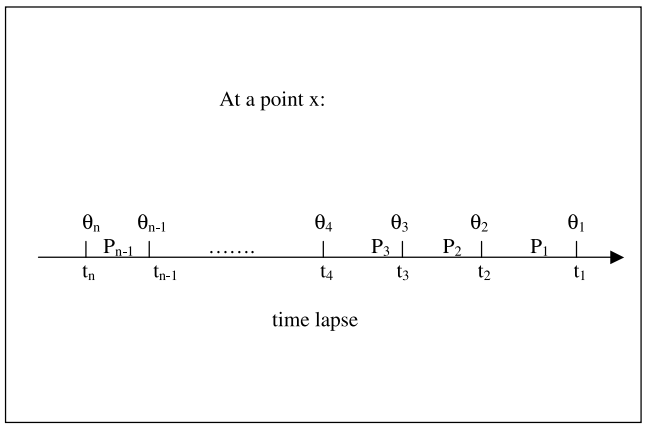

Figure 1. Conceptual example of a time series of soil moisture divided into $n - 1$ periods: the cumulative rainfall during each period is P_i, which is bounded by time t_i and t_{i+1}, and soil moisture at t_i and t_{i+1} are θ_i, and θ_{i+1}, respectively. The subscript for the time is in the opposite direction of the time lapse for convenience.

actual diffusion coefficient due to the overland flow can be less than $\kappa = 10^5$ m^2/hr.

[11] To link soil moisture to cumulative rainfall observations, the rainfall rate $p(x, t)$ is taken to be a constant over short time periods, i.e., $\Delta P(x)/\Delta t$, where $\Delta P(x)$ is the cumulative rainfall during the time period from t to $t + \Delta t$. Substituting $\Delta P(x)/\Delta t$ in equation (2) and dropping the diffusion term, we have:

$$Z\frac{\partial\theta}{\partial t} = -\eta\theta + \gamma\frac{\Delta P(x)}{\Delta t}. \tag{3}$$

Assuming η and γ are independent of time and $\Delta P(x)/\Delta t$ is a constant in the time period from t to $t + \Delta t$, equation (3) is reduced to an ordinary differential equation:

$$\frac{Zd\theta}{-\eta\theta + \gamma\Delta P/\Delta t} = dt \tag{4}$$

[12] Let us consider a time series of soil moisture illustrated in Figure 1 (note the subscript of time is in the opposite direction of the time lapse for convenience). The cumulative rainfall depth is marked for each time period between two adjacent soil moisture measurements. Integrating equation (4) during the time period from t_2 to t_1 gives:

$$\int_{t_2}^{t_1}\frac{Z}{-\eta\theta + \gamma\Delta P/\Delta t}d\theta = \int_{t_2}^{t_1} dt, \tag{5a}$$

$$\frac{Z}{-\eta}\ln\left[\frac{-\eta\theta_1 + \gamma P_1/(t_1 - t_2)}{-\eta\theta_2 + \gamma P_1/(t_1 - t_2)}\right] = t_1 - t_2 \tag{5b}$$

Equation (5b) can be simplified as follows:

$$\theta_1 = \theta_2 e^{-\frac{\eta}{Z}(t_1 - t_2)} + \frac{\gamma P_1/(t_1 - t_2)}{\eta}\left[1 - e^{-\frac{\eta}{Z}(t_1 - t_2)}\right] \tag{6}$$

The similar equations for θ_2, θ_3, …, θ_{n-1} are given by

$$\theta_2 = \theta_3 e^{-\frac{\eta}{Z}(t_2 - t_3)} + \frac{\gamma P_2/(t_2 - t_3)}{\eta}\left[1 - e^{-\frac{\eta}{Z}(t_2 - t_3)}\right] \tag{7}$$

$$\theta_3 = \theta_4 e^{-\frac{\eta}{Z}(t_3 - t_4)} + \frac{\gamma P_3/(t_3 - t_4)}{\eta}\left[1 - e^{-\frac{\eta}{Z}(t_3 - t_4)}\right] \tag{8}$$

$$\theta_{n-1} = \theta_n e^{-\frac{\eta}{Z}(t_{n-1} - t_n)} + \frac{\gamma P_{n-1}/(t_{n-1} - t_n)}{\eta}\left[1 - e^{-\frac{\eta}{Z}(t_{n-1} - t_n)}\right] \tag{9}$$

Substituting equation (7) into (6), we have

$$\begin{aligned}\theta_1 =& \left\{\theta_3 e^{-\frac{\eta}{Z}(t_2 - t_3)} + \frac{\gamma P_2/(t_2 - t_3)}{\eta}\left[1 - e^{-\frac{\eta}{Z}(t_2 - t_3)}\right]\right\} \\ &\cdot e^{-\frac{\eta}{Z}(t_1 - t_2)} + \frac{\gamma P_1/(t_1 - t_2)}{\eta}\left[1 - e^{-\frac{\eta}{Z}(t_1 - t_2)}\right] \\ &= \theta_3 e^{-\frac{\eta}{Z}(t_1 - t_3)} + \frac{\gamma P_2/(t_2 - t_3)}{\eta}\left[1 - e^{-\frac{\eta}{Z}(t_2 - t_3)}\right] \\ &\cdot e^{-\frac{\eta}{Z}(t_1 - t_2)} + \frac{\gamma P_1/(t_1 - t_2)}{\eta}\left[1 - e^{-\frac{\eta}{Z}(t_1 - t_2)}\right]\end{aligned} \tag{10}$$

Performing the same procedure as above, we can derive an equation of θ_1 which only consists of θ_n, P_1, P_2, …, P_{n-1}, which is shown as follows:

$$\begin{aligned}\theta_1 &= \theta_n e^{-\frac{\eta}{Z}(t_1 - t_n)} + \frac{\gamma P_{n-1}/(t_{n-1} - t_n)}{\eta}\left[1 - e^{-\frac{\eta}{Z}(t_{n-1} - t_n)}\right]e^{-\frac{\eta}{Z}(t_1 - t_{n-1})} \\ &\quad + \cdots + \frac{\gamma P_2/(t_2 - t_3)}{\eta}\left[1 - e^{-\frac{\eta}{Z}(t_2 - t_3)}\right]e^{-\frac{\eta}{Z}(t_1 - t_2)} \\ &\quad + \frac{\gamma P_1/(t_1 - t_2)}{\eta}\left[1 - e^{-\frac{\eta}{Z}(t_1 - t_2)}\right]e^{-\frac{\eta}{Z}(t_1 - t_1)} \\ &= \theta_n e^{-\frac{\eta}{Z}(t_1 - t_n)} + \gamma\sum_{i=1}^{n-1}\frac{[P_i/(t_i - t_{i+1})]}{\eta}\left[1 - e^{-\frac{\eta}{Z}(t_i - t_{i+1})}\right]e^{-\frac{\eta}{Z}(t_1 - t_i)} \\ &= \theta_n e^{-\frac{\eta}{Z}(t_1 - t_n)} + \gamma B\end{aligned} \tag{11}$$

where $B = \sum_{i=1}^{n-1}\frac{[P_i/(t_i - t_{i+1})]}{\eta}\left[1 - e^{-\frac{\eta}{Z}(t_i - t_{i+1})}\right]e^{-\frac{\eta}{Z}(t_1 - t_i)}$, represents the summation of the weighted ratio of rainfall rate to loss coefficient. Equation (11) shows that as the window size (i.e., $t_1 - t_n$) increases, the exponential term $e^{-\frac{\eta}{Z}(t_1 - t_n)}$ approaches zero, and thus the contribution of the leading term of the right hand side of equation (11) to θ_1 diminishes. Therefore, at a threshold time window size, we can estimate soil moisture directly from the weighted average cumulative rainfall depth without any information about the initial soil moisture condition. On the other hand, the further beyond t_1, the smaller the precipitation term, and the lower the contribution of the rainfall to the soil moisture at time t_1, which ensures that the solution is stable.

[13] The threshold time window size depends on the value of (η/Z) and the climate condition. For example, if η = 1m/year (from ER94), Z = 0.05m, then for initial soil moistures θ_n varying between hypothetical "dry" (2% vol/vol) and "wet" (50% vol/vol) conditions, the threshold time window size varies between 25 days for the "dry" case and 84 days for the "wet" case. The threshold window corresponds to the time for the first term of the right hand side of

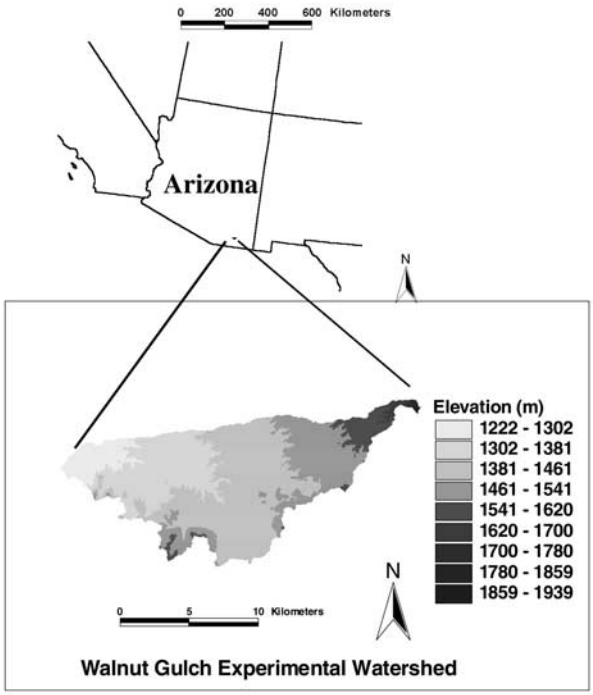

(a) Monsoon'90

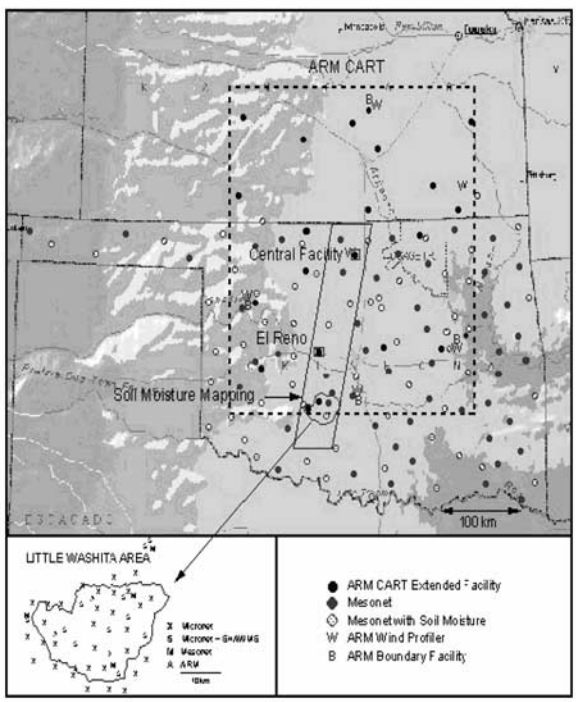

(b) Washita'92 and SGP'97

Figure 2. Location of campaigns studied: (a) Monsoon'90 field experimental domain; (b) SGP'97 field experimental domain. The Little Washita Watershed is inside SGP'97 domain. See color version of this figure at back of this issue.

equation (11) to approach 0.5 (% vol/vol) rendering the contribution of the initial condition to the estimated soil moisture negligible.

3. Study Areas

[14] The soil moisture measurements including ground-measured and remotely sensed observations during three field experiments, Monsoon'90, Washita'92, and SGP'97, are used in this study. In the summer of 1990, the Monsoon'90 large-scale interdisciplinary field experiment was conducted in the Walnut Gulch Experimental Watershed (WGEW) of southeast Arizona (see Figure 2), covering about 148 km^2. During Monsoon'90, a L band Push Broom Microwave Radiometer (PBMR) mounted on a National Aeronautics and Space Administration (NASA) C-130 aircraft was flown at an altitude of 600m above the ground to measure soil moisture [*Schmugge et al.*, 1994]. Six soil moisture images over an 8 $\times$ 20 km^2 area with a 40-m horizontal resolution are available between July 31 and August 10 (i.e., on day 212, 214, 216, 220, and 221). The gravimetric soil moisture was also measured at eight Met-flux stations during Monsoon'90 [*Schmugge et al.*, 1994]. The accumulative rainfall data collected at 112 rain gauges inside WGEW during 1990 can be downloaded from the Monsoon'90 web site (http://hydrolab.arsusda.gov/m90/monsoon90.html).

[15] Washita'92 was an experiment conducted by NASA, United States Department of Agriculture (USDA), and other universities in the Little Washita Watershed of central Oklahoma (see Figure 2). Both conventional measurements (i.e., ground direct measurements) and remotely sensed observations of soil moisture are made from June 10 to June 18. The Electrically Scanned Thinned Array Radiometer (ESTAR) was the sensor used to measure soil moisture [*Jackson and Le Vine*, 1996]. A total of 8 ESTAR-derived soil moisture images with a 200-m horizontal resolution, ground-measured soil moisture, and daily rainfall depth collected at 42 USDA ARS Micronet stations (from 16 May to 30 June 1992) are available from Washita'92 web site (http://hydrolab.arsusda.gov/washita92/wash92.htm).

[16] In the summer of 1997, NASA, USDA and other agencies and universities [*Jackson et al.*, 1999] conducted a larger scale experiment (compared to Monsoon'90 and Washita'92) over the Southern Great Plains that is called SGP'97 (see Figure 2). The main objective of this experiment is to use ESTAR to map daily surface soil moisture over an area greater than 10,000km^2 and a period on an order of one month. Ground-based soil moisture data and 16 ESTAR-derived soil moisture images from 18 June to 16 July 1997 can be downloaded from SGP'97 web site (http://daac.gsfc.nasa.gov/CAMPAIGN_DOCS/SGP97/sgp97.html).

4. Methodology and Results

[17] Equation (11) was applied to each field experimental domain. To compare the estimated soil moisture from rainfall data to the remotely sensed soil moisture images, daily rainfall images were developed from rain gauge measurements or NEXRAD precipitation products. For

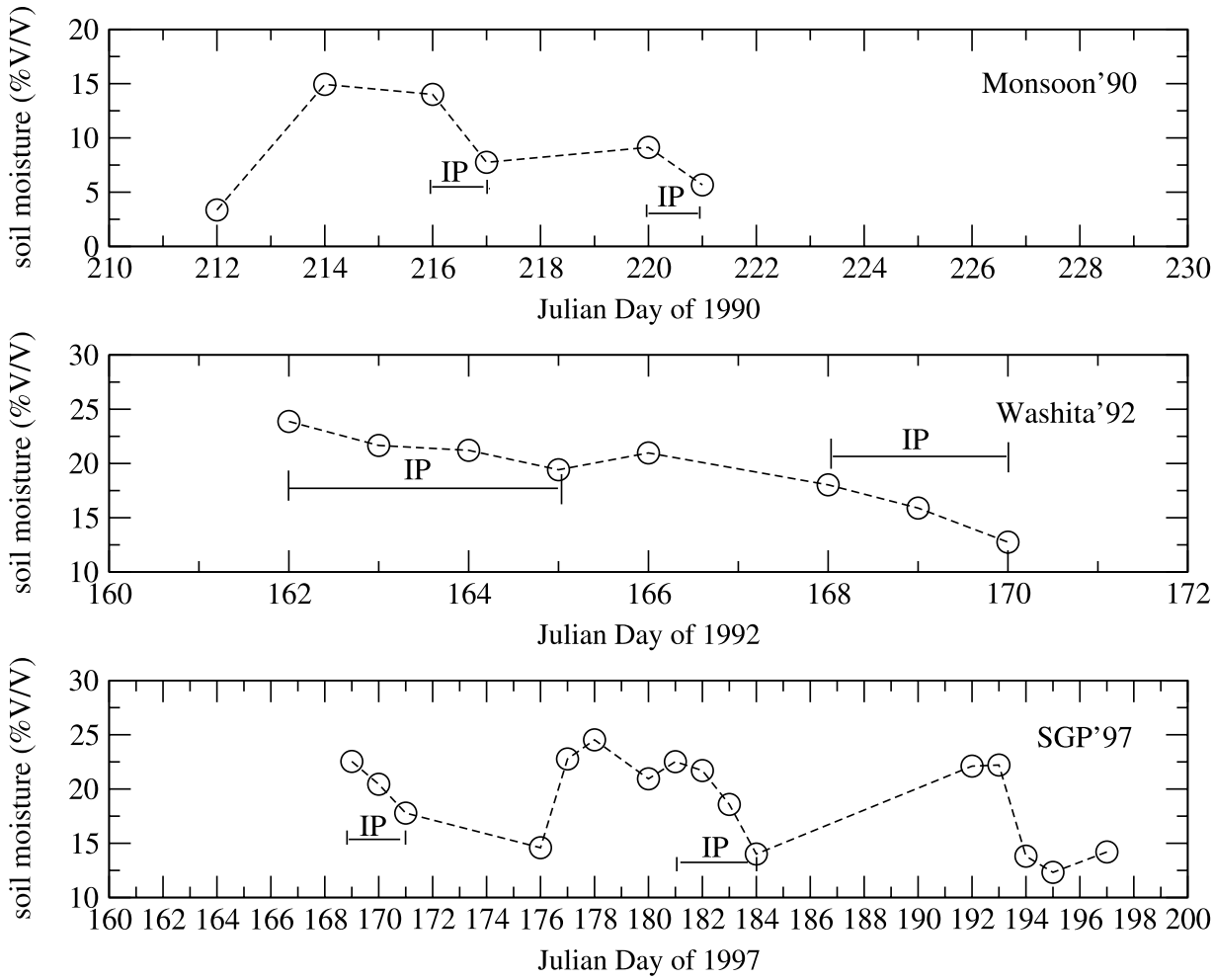

Figure 3. Time series of mean soil moisture estimated by remote sensing during Monsoon'90, Washita'92, and SGP'97. Interstorm periods (IP) are marked on each plot.

Monsoon'90 and Washita'92, we used the inverse distance weighted method to interpolate rainfall depth at each grid based on rain gauge observations. Daily accumulative rainfall maps over the SGP'97 region were constructed from NEXRAD precipitation products developed at Arkansas Red Basin River Forecast Center. To match the projection and the horizontal resolution of ESTAR soil moisture images (i.e., 800-m), the NEXRAD data were reprojected from Polar projection to Universal Transverse Mercator (UTM) projection, zone 14.

4.1. Determination of the Window Size

[18] To apply equation (11) for estimating surface soil moisture, we need first to determine the window size n. Before considering the spatial variation of the loss coefficient η, which will be addressed in the later part of this section, we first assume that η and the infiltration coefficient γ are spatially uniform. Therefore we can estimate η from the time series of mean soil moisture over each domain (see Figure 3). During any interstorm period, taking the areal average of equation (3), we have:

$$Z\frac{\partial\bar{\theta}}{\partial t} = -\eta\bar{\theta} \tag{12}$$

where $\bar{\theta}$ is the mean value of soil moisture over the observed region. The magnitude of η is given by:

$$\eta = -Z\left(\frac{\Delta\bar{\theta}/\Delta t}{\bar{\theta}}\right) \tag{13}$$

where Z = 0.05m for all remotely sensed soil moisture studied in this study.

[19] Using observed soil moisture (Figure 3), two interstorm periods (IP) during each experiment are chosen, Monsoon'90 (day 216-day 217, day 220-day 221), Washita'92 (day 162–day 165, day 168-day 170), and SGP'97 (day 169-day 171, day 181- day 184), for estimating the loss coefficient. We use the mean value of estimated loss coefficient η for all regions, which is 3.5 m/year. This loss coefficient value reduces the required window size compared to the loss coefficient 1.0 m/year, since a higher loss coefficient makes each exponential term in equation (11) decay faster than a smaller loss coefficient. We temporarily leave the value of γ undetermined, since each term with cumulative rainfall in equation (11) is multiplied by γ.

[20] To test this method and determine the threshold of window size, we use the least squares method to fit the scatterplots of spatial mean of the estimated soil moisture (actually it is the mean of B defined in equation (11)) from

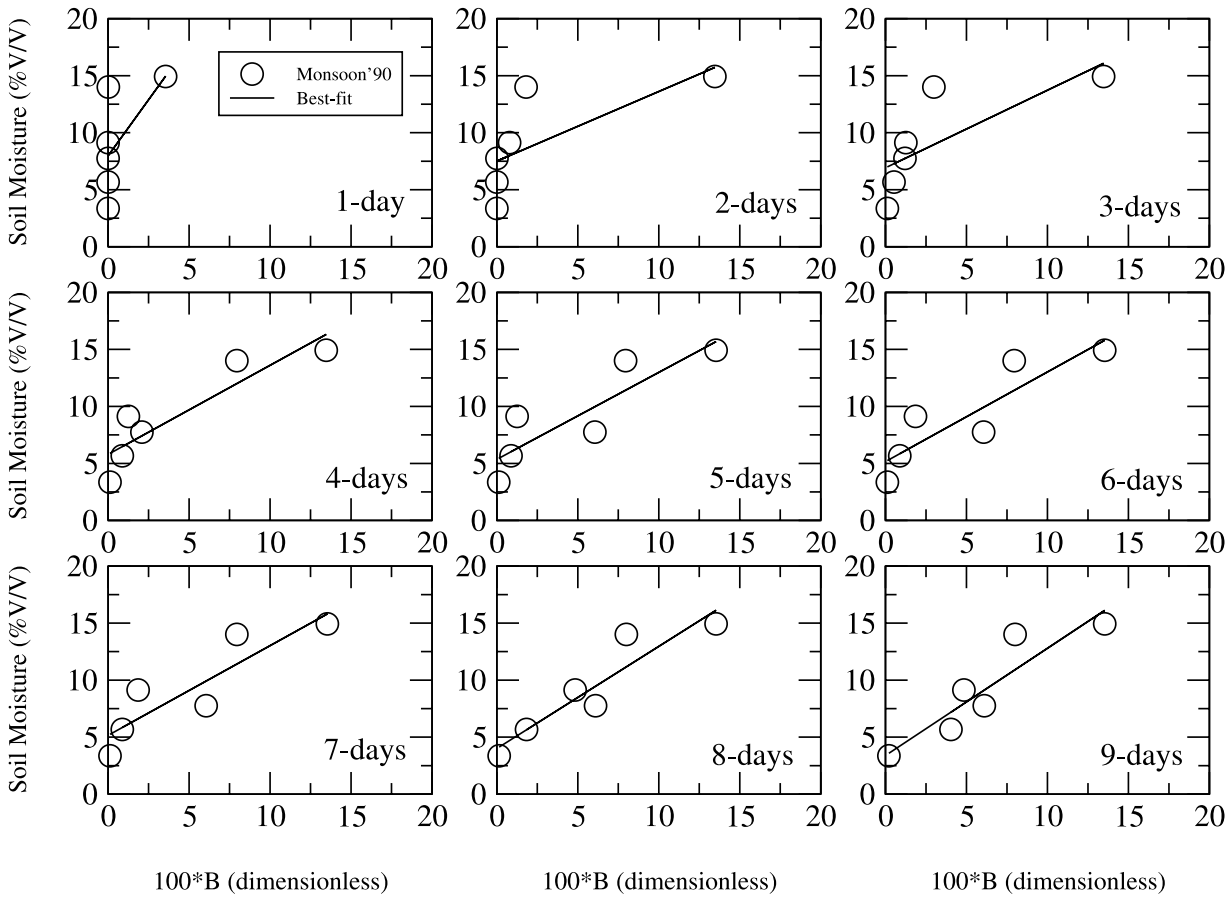

Figure 4. Scatterplots of mean soil moisture versus mean B (defined in equation (11)) value under different time window size (i.e., 1-day, 2-days, . . ., 9-days) over the Monsoon'90 region. The loss coefficient used here is 3.5 m/year.

rainfall versus spatial mean of the remotely sensed soil moisture and compute the Root Mean Squared Error (RMSE). Figure 4 shows an example for Monsoon'90. The plot of RMSE versus window size shown in Figure 5 demonstrates that when window size is less than one week, the results are not stable. After one week, as window size increases, the RMSE decreases, and approaches a stable value. Although only about 26 serial daily rainfall maps are available for Washita'92, the results become stable as window size reaches 14 days. Therefore, if the loss coefficient is 3.5 m/year, the 14-day window size is the threshold size for us to determine soil moisture by using equation (11).

[21] As mentioned in section 1, *Findell and Eltahir* [1997] used a 21-day moving average of rainfall, and found no significant correlation between the moving average rainfall and soil moisture. To explain this, we also applied the least squares method to fit the moving average rainfall versus spatial mean of remotely sensed soil moisture, and computed the RMSE. The plots of window size versus RMSE for each case are also shown in Figure 5. The unstable behavior associated with the moving average method is clearly shown in Figure 5, no matter which window size is chosen. Unlike equation (11), since no exponential decay factor is involved in computing the moving average of rainfall, the contribution from the rainfall at any time inside the window is the same, which creates the unstable behavior of the solutions. Therefore different window sizes give a different correlation between moving average rainfall and soil moisture: at some window sizes the correlation may be high, while at others the correlation may be low.

4.2. Determination of the Infiltration Coefficient

[22] To estimate soil moisture by using equation (11), we also need to determine the infiltration coefficient γ based on the relationship between mean soil moisture and the mean B value. Since the observed domain-mean values of soil moisture over the three field experiments only varied between 0 (% vol/vol) and 30 (% vol/vol), while the whole dynamical range of soil moisture could be from 0 (% vol/vol) to the maximum porosity (55% vol/vol), we also compute mean soil moisture and mean B values for 7 catchments inside the SGP'97 domain (see Figure 6). A strong correlation between mean soil moisture and mean B appears in Figure 7. However, in contrast to the linear relationship between B and θ indicated by equation (11), the relationship shown in Figure 7 is not linear. According to equation (11) the slope of the $B \sim \theta$ curve is the infiltration coefficient γ. In reality, as B increases, soil moisture increases and finally approaches saturated soil moisture, and the infiltration coefficient γ (or the slope of the $B \sim \theta$ curve) will decrease and finally approach zero.

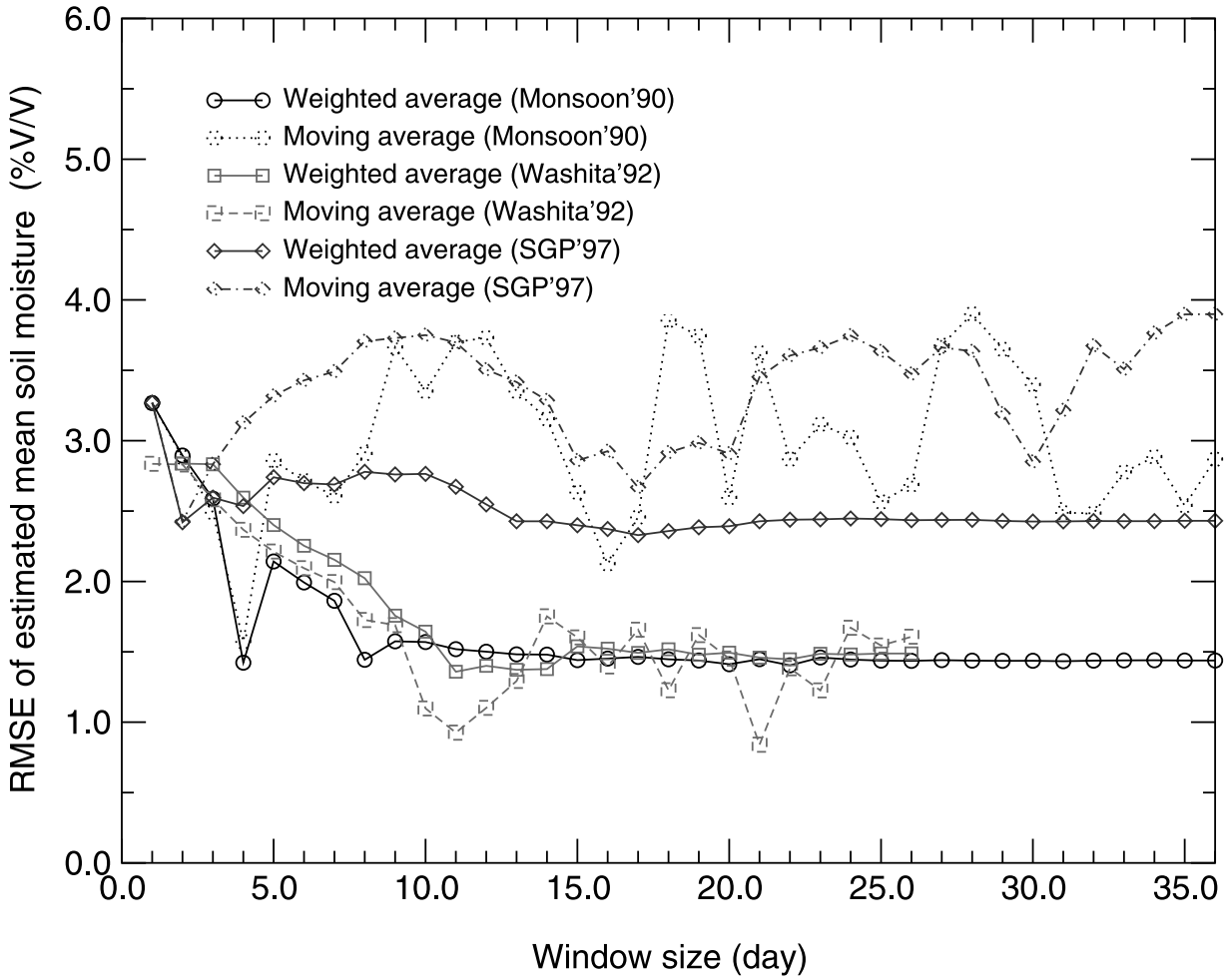

Figure 5. Plot of root mean squared error (RMSE) of the estimated mean soil moisture from rainfall observations versus window size. The loss coefficient is 3.5 m/year for the time-weighted averaging. See color version of this figure at back of this issue.

The decline of the infiltration coefficient with increasing of B is the main reason for the nonlinear pattern shown in Figure 7. Such nonlinearity indicates that when we apply equation (11) to predict soil moisture, we need to determine the infiltration coefficient according to the range of B values (e.g., γ_1 for $0 \leq B \leq 1.0$, γ_2 for $1.0 < B \leq 2.0$, and etc).

[23] To make this method practically simple and useful, according to the shape of the $B \sim \theta$ curve, we assume the relationship between B and soil moisture satisfies the following equation:

$$\theta = 0.55\left(1 - e^{-cB}\right) \tag{14}$$

where θ has the dimensions of vol/vol. Under this assumption, the infiltration coefficient γ loses its role in determining soil moisture, since we only need to compute the B value, and substitute B into equation (14) for computing soil moisture. The parameter c in equation (14) is a constant that can be determined by fitting equation (14) to the scatterplots shown in Figure 7. The resulting c is 0.976, and the root mean squared error of the estimated soil moisture is 0.05 vol/vol. The correlation coefficient between the observed and estimated mean soil moisture is 0.83.

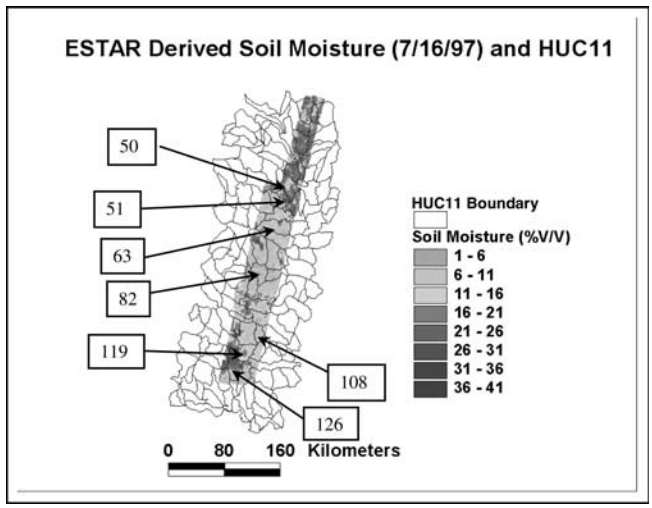

Figure 6. Seven catchments inside SGP'97 domain are used for linking mean soil moisture to mean B values. Map of USGS hydrologic unit code (HUC) with 11 digits is overlapped by Electrically Scanned Thinned Array Radiometer (ESTAR)-derived soil moisture on 7/16/1997 (16 July 1997). The numbers inside the boxes are indices of seven catchments. See color version of this figure at back of this issue.

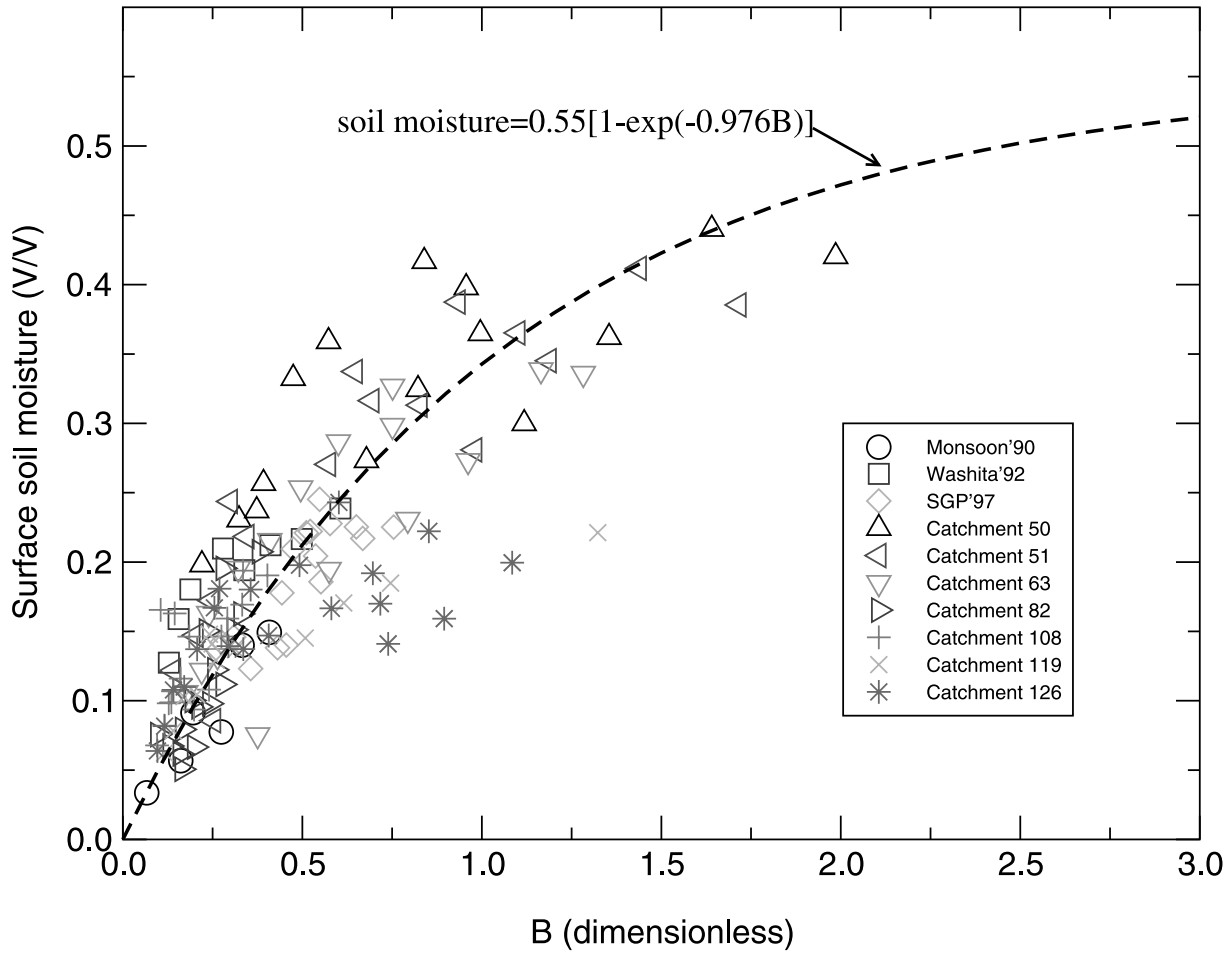

Figure 7. Relation between observed mean soil moisture and mean B values over the Monsoon'90, Washita'92, SGP'97 domains, and seven catchments inside the SGP'97 domain. The dashed line is the empirical relationship between soil moisture and B value. See color version of this figure at back of this issue.

4.3. Spatial Variability of the Loss Coefficient

[24] Although mean soil moisture can be estimated from the above method, the spatial structures of soil moisture may not be fully recovered, because the spatial variation of η is neglected, and the spatial variation of soil and land cover has not been taken into account. To estimate the loss coefficient, the ground-measured soil moisture during Monsoon'90 and Washita'92 are used. The observed surface soil moisture and characteristics of each ground site are given by *Schmugge et al.* [1994] (for Monsoon'90) and at hydrolab.arsusda.gov/washita92/wash92.htm (for Washita'92). The scatterplots of land surface characteristics versus the estimated loss coefficient are shown in Figure 8. There exist some trends among the loss coefficient and soil properties. The loss coefficient increases as saturated hydraulic conductivity increases and as porosity and field capacity decrease. To simplify the regression equation, saturated hydraulic conductivity and leaf area index (LAI) are chosen as two independent variables for determining the loss coefficient by using linear multiple regression. Figure 8 also shows that most of the loss coefficients in Monsoon'90 region are greater than those in Washita'92 domain, which may be due to differences in climate. Therefore the empirical formula of the loss coefficient is determined region by region. The resulting loss coefficient functions are given by

Monsoon'90

$$\eta = \begin{cases} 4.479 + 0.386K_s - 0.322\text{LAI}, \\ 1, \quad \text{if} \quad (4.479 + 0.386K_s - 0.322\text{LAI} < 1) \end{cases} \tag{15a}$$

Washita'92

$$\eta = \begin{cases} 2.220 + 0.146K_s - 0.186\text{LAI} \\ 1, \quad \text{if} \quad (2.220 + 0.146K_s - 0.186\text{LAI} < 1) \end{cases} \tag{15b}$$

where K_s is in cm/hr, and η is in m/year. The RMSEs of the estimated loss coefficient are 0.83m/year and 0.89m/year, and the correlation coefficients are 0.52 and 0.51 for Monsoon'90 and Washita'92, respectively. The scatterplot of the estimated loss coefficients based on equation (15) versus the estimated loss coefficient directly from ground-measured soil moisture is shown in Figure 9. The derived formula given in (15) is consistent with the physics related to the loss coefficient, i.e., a large loss coefficient is associated with a fast drainage (i.e., large K_s) and a strong

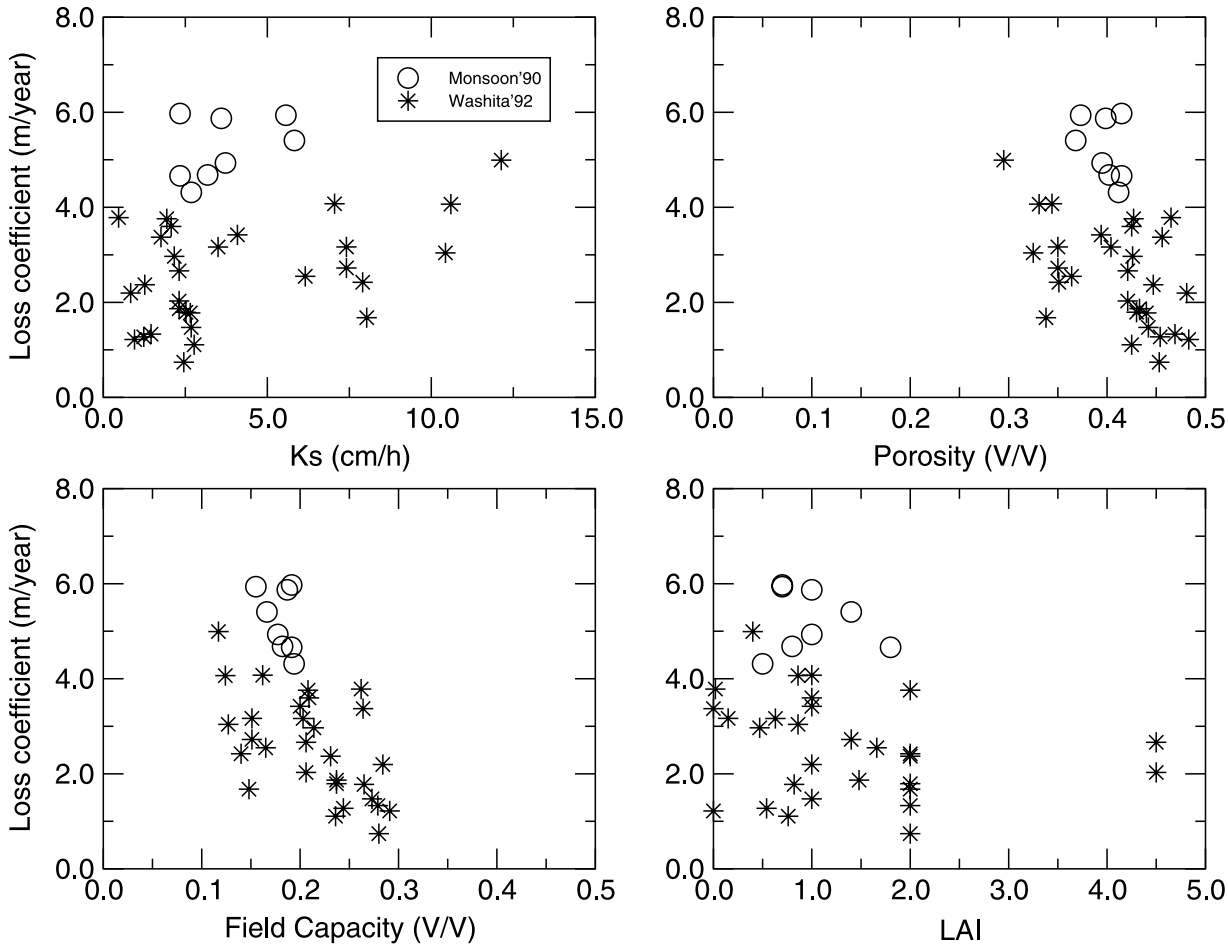

Figure 8. Relation between the loss coefficient and selected land surface characteristics at Metflux stations during Monsoon'90 and ground sampling sites during Washita'92.

evaporation directly from surface soil rather than from the vegetation cover (i.e., small LAI).

4.4. Errors in the Estimated Surface Soil Moisture

[25] Combining soil texture maps and LAI images over each region, we can develop a loss coefficient map by using the empirical formula (15). Since the Washita'92 domain is inside the SGP'97 region, the formula for Washita'92 is also applied to SGP'97 domain. The loss coefficient maps are shown in Figure 10. With those loss coefficient maps, we can retrieve surface soil moisture at each pixel based on equations (11) and (14). Figure 11 shows the estimated soil moisture images using a window size of 14-days for selected days over each domain. For comparison, remotely sensed soil moisture images on the same selected days are also shown in Figure 11.

[26] Figure 11 demonstrates that the proposed method can capture some of the spatial structure of soil moisture fields, especially over SGP'97 domain, although the loss coefficient function used for SGP'97 domain was derived from ground soil moisture measurements during Washita'92. On day 178, 1997, the wet patterns in the northern part of the SGP'97 region, and the dry patterns near the center of the domain shown on the ESTAR soil moisture image were also captured by the proposed simple method. The predicted soil moisture over Washita'92 domain appears wetter than the ESTAR soil moisture, which indicates that the loss coefficient is underestimated. The underestimation of the loss coefficient is possibly due to the uncertainty in soil saturated hydraulic conductivity and LAI.

[27] To examine the accuracy of the estimated soil moisture, we calculated RMSE and correlation coefficients against remotely sensed soil moisture maps for each pixel for Monsoon'90, Washita'92, and SGP'97 (see Table 1). The errors in the estimated soil moisture are close to those of remotely sensed soil moisture for Monsoon'90 (2% vol/vol), and Washita'92 (10% vol/vol). Although the magnitude of the errors for SGP'97 is around 10 (% vol/vol), which is higher than the error of ESTAR soil moisture (3% vol/vol), almost all of the correlation coefficients are greater than 0.5. This indicates that the suggested model has ability to retrieve surface soil moisture.

[28] To understand how the errors in the estimated soil moisture vary with dry-down and wetting processes, we plot mean observed soil moisture versus RMSE and correlation coefficient for all three domains (see Figure 12). Large errors during wet periods shown in Figure 12 may be due to the uncertainty in the rainfall measurements. However, the relatively high correlation coefficients during wet periods imply that the errors in the rainfall measurements used in this study are small, and not the main reason for the large RMSE of the estimated soil moisture. There-

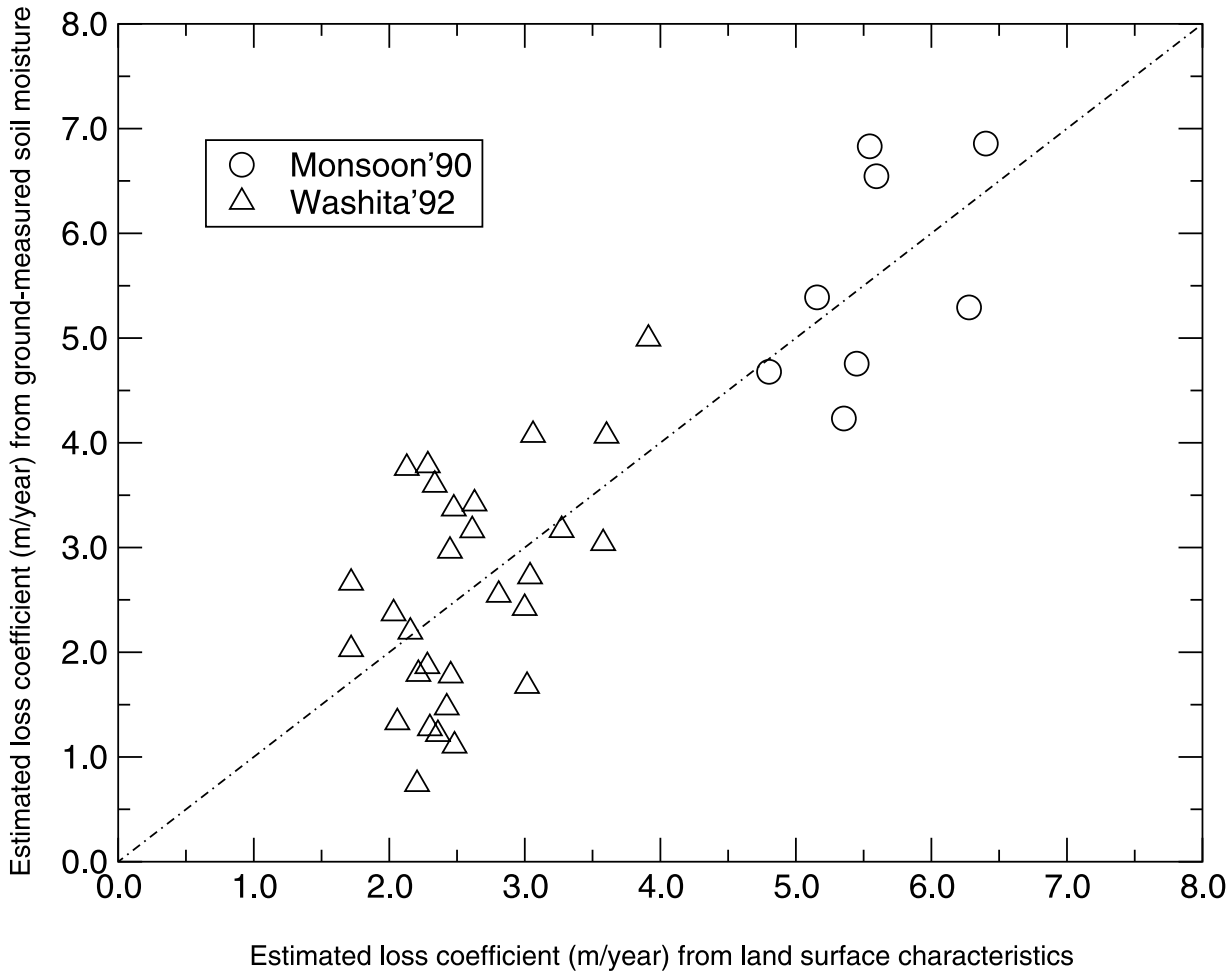

Figure 9. Scatterplot of the estimated loss coefficients from land surface characteristics based on equation (15) versus the estimated loss coefficients directly from ground-measured soil moisture over Monsoon'90 and Washita'92 regions.

fore the sources of the errors are the relationship between B and soil moisture ($\theta = 0.55(1 - e^{-cB})$) and the loss coefficient.

[29] The relationship between B and soil moisture has two ends. At the lower end, B approaches zero and soil moisture approaches zero; and at the higher end, B approaches a threshold and soil moisture approaches porosity. In this study, we only use one relationship between soil moisture and B to represent all pixels in Monsoon'90, Washita'92, and SGP'97. However, the heterogeneity of soil texture determines that using only one relationship will definitely introduce a large error during wet periods, but not during dry periods, because all soil moisture versus B curves should approach the same lower end (i.e., dry condition, $B \rightarrow 0$, $\theta \rightarrow 0$), but not the same upper end, since the upper ends depend on soil hydraulic properties.

[30] Figure 12 also shows that the correlation coefficients are related to the spatial resolution of remotely sensed soil moisture maps, i.e., a higher resolution soil moisture map associated with a lower correlation coefficient (e.g., Monsoon'90: 40-m resolution and Washita'92: 200-m), and verse versa (e.g., SGP'97: 800-m). There are two possible reasons: (1) using only one relationship between soil moisture and B reduces the ability of this simple method to capture the spatial patterns of soil moisture shown on remotely sensed high resolution soil moisture images; (2) the uncertainties in land cover and soil texture maps produce the errors in the loss coefficient maps.

[31] Recalling equation (1), the loss term is the combination of evaporation/evapotranspiration and drainage. Therefore the loss coefficient should be a function of land cover, soil properties and weather conditions. In this study we neglected the effects of atmospheric conditions on the loss coefficient, because the time period of the remotely sensed soil moisture data used in this study is less than 1 month. Although the variation of daily weather conditions (i.e., wind, air temperature, relative humidity, solar radiation) during one month is small, except for cloud conditions, the cloud conditions can affect the loss coefficient significantly, because the downward solar radiation reaching the ground is directly controlled by cloud conditions.

[32] There are two other factors that may be also responsible for the errors in the estimated soil moisture. All soil and vegetation characteristics used in this study for determination of the loss coefficient come from lookup tables, which are subject to errors and uncertainties. We neglect the

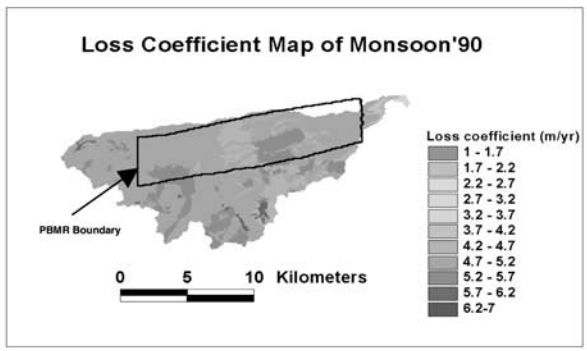

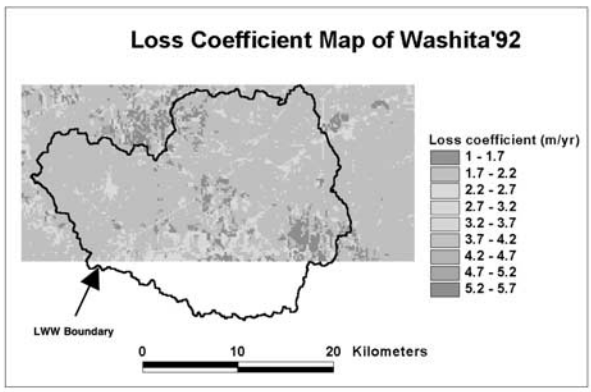

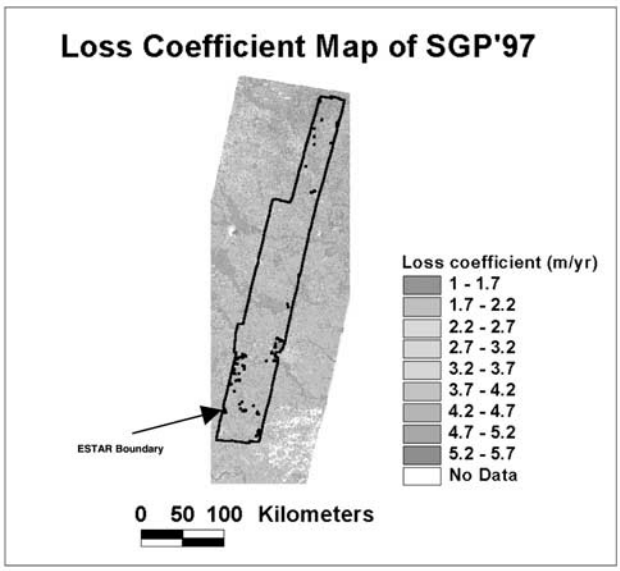

Figure 10. Loss coefficient maps of Monsoon'90, Washita'92, and SGP'97 estimated by equation (15). (PBMR stands for Push Broom Microwave Radiometer and LWW stands for Little Washita Watershed). See color version of this figure at back of this issue.

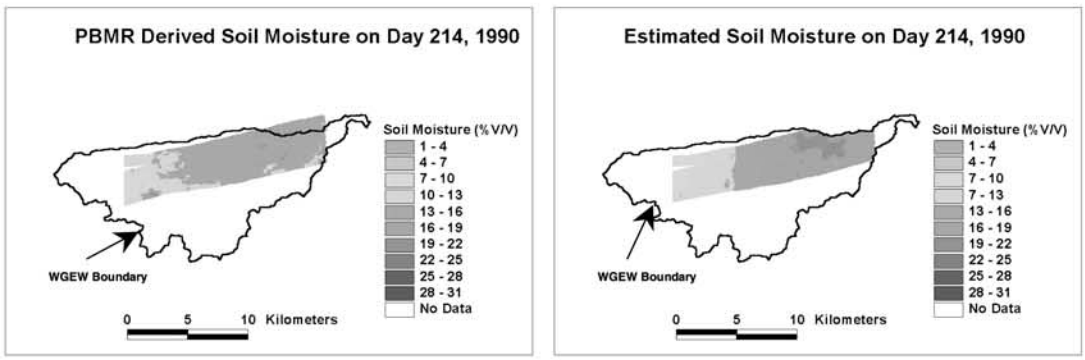

(a) Monsoon'90

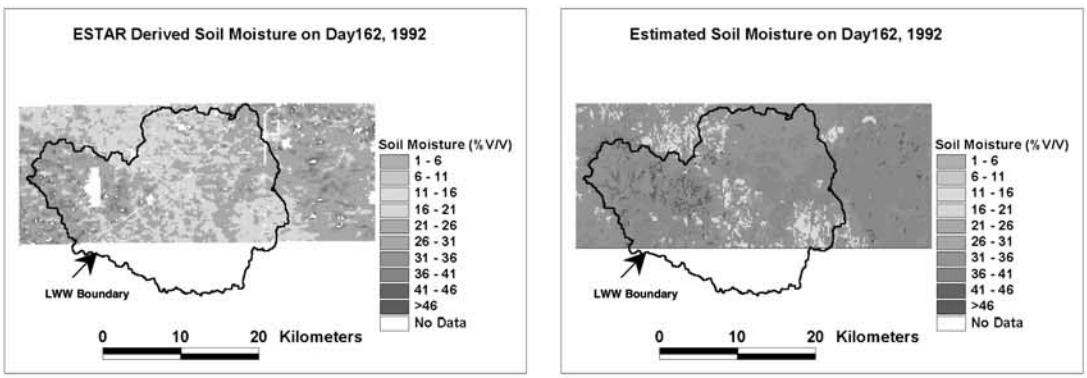

(b) Washita'92

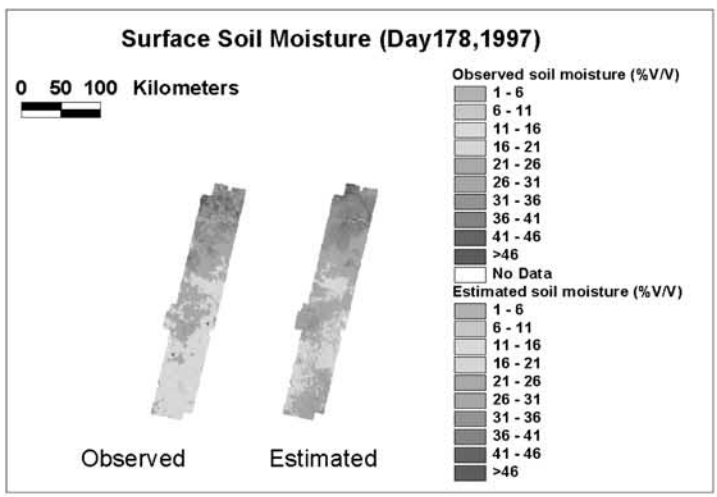

(c) SGP'97

Figure 11. (a) PBMR-derived and estimated soil moisture on day 214 during Monsoon'90; (b) ESTAR-derived and estimated soil moisture on day 162 during Washita'92; (c) ESTAR-derived and estimated soil moisture on day 178 during SGP'97. See color version of this figure at back of this issue.

Table 1. Statistical Comparison of Estimated Soil Moisture With Remotely Sensed Soil Moisture Pixel by Pixel for Three Intensive Field Campaigns: Monsoon'90, Washita'92, and SGP'97[a]

Monsoon'90			Washita'92			SGP'97		
Day	RMSE	r	Day	RMSE	r	Day	RMSE	r
212	2.54	0.43	161	13.24	0.38	169	10.17	0.53
214	1.77	0.77	162	12.71	0.40	170	9.89	0.56
216	2.97	0.45	163	11.10	0.43	171	11.01	0.60
217	2.09	0.43	164	10.54	0.43	176	7.24	0.54
220	2.41	0.41	165	7.87	0.43	177	8.12	0.70
221	1.25	0.45	167	6.86	0.42	178	7.87	0.76
			168	6.89	0.42	180	7.01	0.64
			169	7.78	0.38	181	8.21	0.84
						182	7.22	0.88
						183	10.38	0.82
						184	10.40	0.86
						192	10.10	0.46
						193	9.49	0.56
						194	10.76	0.53
						195	10.56	0.47
						197	9.00	0.48

[a]RSME is root square mean error, and r is correlation coefficient.

interception by the canopy in equation (2), which may introduce a large error especially over forest regions, although interception losses may partially explain the counterintuitive result that our empirical loss coefficients decrease with increasing LAI. In addition, it is relatively easy to solve this problem by including the interception term in the expression of B, given as follows:

$$B = \sum_{i=1}^{n-1} \frac{[(P_i - L_i)/(t_i - t_{i+1})]}{\eta} \left[1 - e^{-\frac{\eta}{Z}(t_i - t_{i+1})}\right] e^{-\frac{\eta}{Z}(t_1 - t_i)} \quad (16)$$

where L_i is the interception in the time period from t_{i+1} to t_i.

5. Conclusions

[33] A simple analytical method for estimating soil moisture directly from rainfall data is proposed and studied. A diagnostic soil moisture equation is derived from the linear stochastic partial differential equation, first proposed by *Entekhabi and Rodriguez-Iturbe* [1994], by dropping the diffusion term. The derived soil moisture is a function of the time-weighted average of previous cumulative rainfall over a period (e.g., >14 days), rather than a moving average of previous cumulative rainfall. Although the concept behind this method is similar to the API method [*Saxton and Lenz*, 1967], this method is directly derived from soil moisture dynamic equation. On the other hand, it overcomes three weaknesses involved in the API method: (1) no initial condition of soil moisture is needed, because as the window size increases, the contribution of the associated cumulative rainfall to the current soil moisture decays due to dry-down processes (i.e., evapotranspiration and percolation); (2) it can be applied to the whole dynamic range of soil moisture,

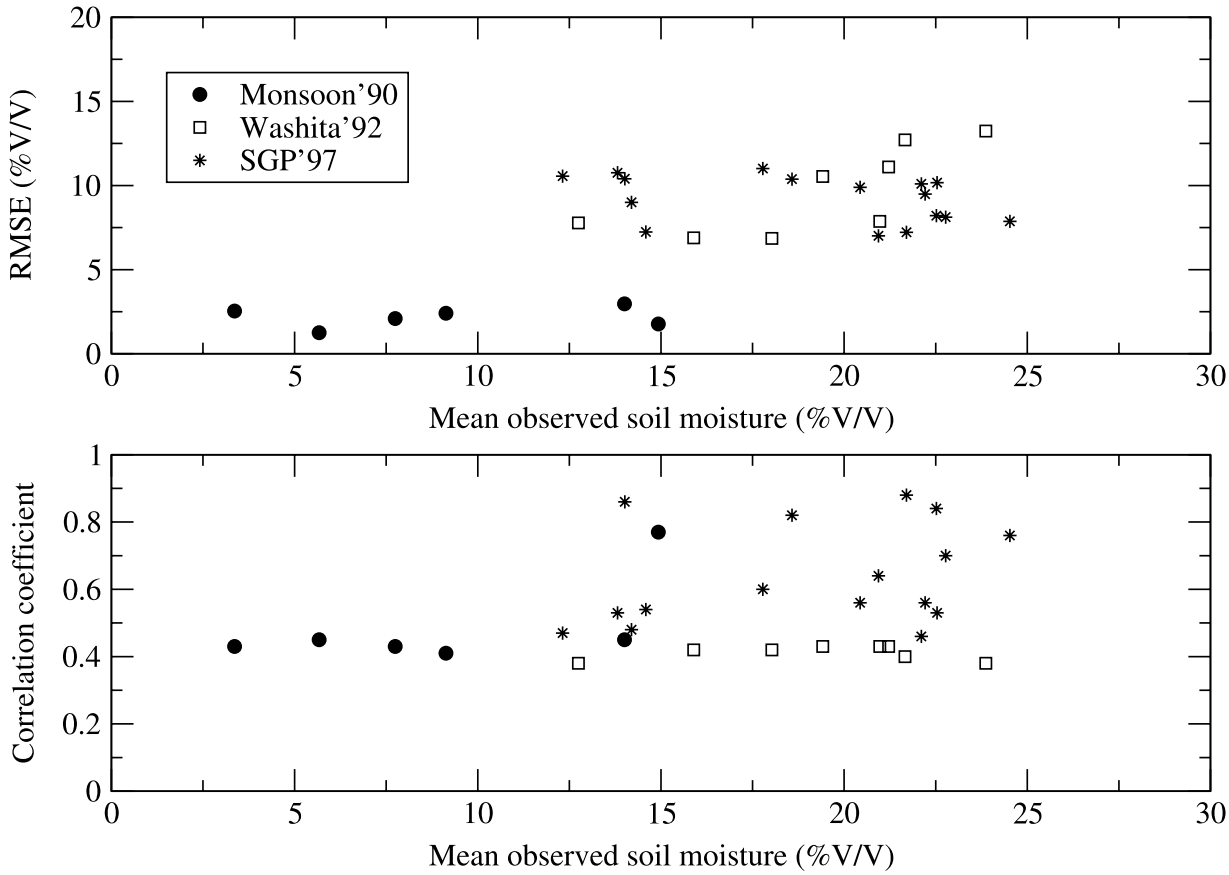

Figure 12. Relation between mean observed soil moisture and (top) RMSEs and (bottom) correlation coefficients for all three domains.

because an exponential relationship between the time-weighted of the ratio of rainfall to the loss coefficient (i.e., B) and soil moisture is introduced, i.e., as B reaches a threshold, soil becomes saturated; and (3) it can predict soil moisture at any time.

[34] The method for estimating a loss coefficient is critical for this method. In this study, we have shown that the loss coefficient can be determined from land surface and soil characteristics. Through comparisons of observed and estimated soil moisture during three field experiments, it is shown that the proposed method is simple and able to capture some spatial and temporal structures of soil moisture fields. The errors in the estimated soil moisture are partially due to neglecting spatial and temporal variation of atmospheric conditions and solar radiation when we compute the loss coefficient. More research on the loss coefficient is needed for eventually developing a loss coefficient function that depends on soil, vegetation, and atmospheric conditions.

[35] As we discussed in section 4.4, using only one relationship between B and soil moisture could produce a large error in the estimated soil moisture, especially during wet periods. Therefore, before we apply this simple method to any location, further effort is needed to develop a family of B versus soil moisture functions that depend on soil hydraulic properties. On the other hand, without considering capillary rise, we could underestimate soil moisture especially where the water table is close to surface, because when B is equal to zero, soil moisture is also zero according to equation (14). It seems that capillary rise does not contribute much to surface soil moisture in our study areas. One possible reason is that water table is deep. Preliminary results from analyzing ground-measured soil moisture data taken at Soil Climate Analysis Network (SCAN) sites (http://www.wcc.nrcs.usda.gov/scan) managed by Natural Resources Conservation Service (NRCS) of United States Department of Agriculture (USDA) indicate that a general relationship between B and soil moisture can be given as:

$$\theta = c_1 + \theta_r + (\phi - \theta_r - c_1)\left(1 - e^{-c_2 B}\right) \qquad (17)$$

where c_1 is the contribution to the surface soil moisture due to capillary rise, θ_r is residual soil moisture content, ϕ is saturated soil moisture content, and c_2 is a parameter related to soil hydraulic properties. This work will be discussed in a forthcoming paper.

[36] Although significant progress has been made in the microwave remote sensing of soil moisture [e.g., *Jackson and Schmugge*, 1989; *Engman*, 1990, 1995], the attenuation of microwave signals by dense canopies [*Ulaby and Wilson*, 1985] makes the soil moisture measurements in forest regions unreliable [*Njoku*, 1999]. Unlike remote sensing of soil moisture, vegetation covers do not produce any adverse effects on remote sensing of rainfall above canopies. With increasing global precipitation measurements (e.g., TRMM, NASA Global Precipitation Measurement (GPM) and land surface characteristic observations (e.g., AVHRR, Landsat, MODIS), this simple diagnostic method could become very useful for retrieving surface soil moisture especially over forests, from a remote sensing point of view.

[37] **Acknowledgments.** The authors would like to thank A. P. Georgakakos, P. J. Hanson, P. J. Mulholland, A. W. King, and two anonymous referees for their valuable comments and suggestions. This research was supported by NASA grant NAG5-8698 (PI: Peters-Lidard) entitled ''Quantifying the relationship between remotely sensed and modeled soil moisture" at Georgia Institute of Technology, and in part by a fellowship with the Oak Ridge National Laboratory (ORNL) Postdoctoral Research Associates Program (F. Pan) which is sponsored by ORNL and administered jointly by ORNL and by the Oak Ridge Institute for Science and Education under contract numbers DE-AC05-84OR21400 and DE-AC05-76OR00033, respectively. This research was also supported by the U.S Department of Energy's Office of Science and performed at ORNL. ORNL is managed by UT-Battelle, LLC, for the U.S Department of Energy under contract DE-AC05-00OR22725. The research described in this article has also been funded in part by an interagency agreement to NASA (Peters-Lidard) from USDA/ARS and USACE. This support is gratefully acknowledged.

References

Betts, A. K., J. H. Ball, and A. C. M. Beljaars, Comparison between the land surface response of the ECMWF model and the FIFE-1987 data, *Q. J. R. Meteorol. Soc.*, *119*, 975–1001, 1993.

Blanchard, B. J., M. J. Mcfarland, T. J. Schmugge, and E. Rhoades, Estimation of soil-moisture with API algorithms and microwave emission, *Water Resour. Bull.*, *17*, 767–774, 1981.

Capehart, W. J., and T. N. Carlson, Estimating near-surface soil moisture availability using a meteorologically driven soil water profile model, *J. Hydrol.*, *160*, 1–20, 1994.

Castelli, F., and I. Rodriguez-Iturbe, Soil moisture-atmosphere interaction in a moist semigeostrophic model of baroclinic instability, *J. Atmos. Sci.*, *52*, 2152–2159, 1995.

Choudhury, B. J., and B. J. Blanchard, Simulating soil water recession coefficients for agricultural watersheds, *Water Resour. Bull.*, *19*, 241–247, 1983.

Dastoor, A., and T. N. Krishnamurti, The landfall and structure of a tropical cyclone: The sensitivity of model predictions to soil moisture parameterizations, *Boundary Layer Meteorol.*, *55*(4), 345–380, 1991.

Delworth, T., and S. Manabe, Climate variability and land surface processes, *Adv. Water Resour.*, *16*, 3–20, 1993.

Dinar, A., K. C. Knapp, and J. D. Rhoades, Production function for cotton with dated irrigation quantities and qualities, *Water Resour. Res.*, *22*, 1519–1525, 1986.

Dingman, S. L., *Physical Hydrology*, Prentice-Hall, Old Tappan, N. J., 575 pp., 1994.

Ducharne, A., R. D. Koster, M. J. Suarez, M. Stieglitz, and P. Kumar, A catchment-based approach to modeling land surface processes in a general circulation model: 2. Parameter estimation and model demonstration, *J. Geophys. Res.*, *105*(D20), 24,823–24,838, 2000.

Engman, E. T., Progress in microwave remote sensing of soil moisture, *Can. J. Remote Sens.*, *16*, 6–14, 1990.

Engman, E. T., Recent advances in remote sensing in hydrology, *U.S. Natl. Rep. Int. Union Geod. Geophys. 1991–1994*, *Rev. Geophys.*, *33*, 967–975, 1995.

Entekhabi, D., and I. Rodriguez-Iturbe, Analytical framework for the characterization of the space-time variability of soil moisture, *Adv. Water Resour.*, *17*, 35–45, 1994.

Farago, T., Soil moisture content: Statistical estimation of its probability distribution, *J. Clim. Appl. Meteorol.*, *24*(4), 371–376, 1985.

Fecan, F., B. Marticorena, and G. Bergametti, Parametrization of the increase of the aeolian erosion threshold wind friction velocity due to soil moisture for arid and semi-arid areas, *Ann. Geophys.*, *17*(1), 149–157, 1999.

Findell, K. L., and E. A. B. Eltahir, An analysis of the soil moisture-rainfall feedback based on direct observations from Illinois, *Water Resour. Res.*, *33*, 725–735, 1997.

Govers, G., Time-dependency of runoff velocity and erosion: the effect of the initial soil moisture profile, *Earth Surf. Processes Landforms*, *16*(8), 713–729, 1991.

Hong, S., and H. Pan, Impact of soil moisture anomalies on seasonal, summertime circulation over North America in a regional climate model, *J. Geophys. Res.*, *105*(D24), 29,625–29,634, 2000.

Hornberger, G. M., et al., A plan for a new science initiative on the global water cycle, 118 pp., U.S. Global Change Res. Program, Washington, D. C., 2001.

Houser, P. R., Remote-sensing soil moisture using four-dimensional data assimilation, Ph.D. thesis, Dep. of Hydrol. and Water Resour., Univ. of Ariz., Tucson, 1996.

Jackson, T. J., and D. M. Le Vine, Mapping surface soil moisture using an aircraft-based passive microwave instrument: Algorithm and example, *J. Hydrol.*, *184*, 85–99, 1996.

Jackson, T. J., and T. J. Schmugge, Passive microwave remote sensing system for soil moisture: Some supporting research, *IEEE Trans. Geosci. Remote Sens.*, *27*, 225–235, 1989.

Jackson, T. J., D. M. Le Vine, A. Y. Hsu, A. Oldak, P. J. Starks, C. T. Swift, J. D. Isham, and M. Haken, Soil moisture mapping at regional scales using microwave radiometry: The Southern Great Plains Hydrology Experiment, *IEEE Trans. Geosci. Remote Sens.*, *37*, 2136–2151, 1999.

Koster, R. D., M. J. Suarez, A. Ducharne, M. Stieglitz, and P. Kumar, A catchment-based approach to modeling land surface processes in a general circulation model: 1. Model structure, *J. Geophys. Res.*, *105*(D20), 24,809–24,822, 2000.

Lindberg, S. E., et al., Increases in mercury emissions from desert soils in response to rainfall and irrigation, *J. Geophys. Res.*, *104*(D17), 21,879–21,888, 1999.

Lynn, B. H., D. Rind, and R. Avissar, The importance of mesoscale circulations generated by subgrid-sale landscape heterogeneities in general circulation models, *J. Clim.*, *8*, 191–205, 1995.

Mahfouf, J.-F., E. Richard, and P. Mascart, The influence of soil and vegetation on the development of mesoscale circulations, *J. Clim. Appl. Meteorol.*, *26*(11), 1483–1495, 1987.

McCumber, M. C., and R. A. Pielke, Simulation of the effects of surface fluxes of heat and moisture in a mesoscale numerical model: 1. Soil layer, *J. Geophys. Res.*, *86*(C10), 9929–9938, 1981.

Mehrotra, R., Sensitivity of runoff, soil moisture and reservoir design to climate change in central Indian river basins, *Clim. Change*, *42*, 725–757, 1999.

Njoku, E. G., AMSR land surface parameters, algorithm theoretical basis document, version 3.0, Jet Propul. Lab., Calif. Inst. of Technol., Pasadena, CA., 1999.

Ookouchi, Y., M. Segal, R. C. Kessler, and R. A. Pielke, Evaluation of soil moisture effects on the generation and modification of mesoscale circulations, *Mon. Weather Rev.*, *112*, 2281–2292, 1984.

Quinn, P., K. Beven, and A. Culf, The introduction of macroscale hydrological complexity into land surface atmosphere models and the effect on planetary boundary layer development, *J. Hydrol.*, *166*, 421–444, 1995.

Saxton, K. E., and A. T. Lenz, Antecedent retention indexes predict soil moisture, *J. Hydraul. Div. Proc. Am. Soc. Civ. Eng.*, *93*, 223–241, 1967.

Schmugge, T., T. J. Jackson, W. P. Kustas, R. Roberts, R. Parry, D. C. Goodrich, S. A. Amer, and M. A. Weltz, Push broom microwave radiometer observations of surface soil moisture in Monsoon'90, *Water Resour. Res.*, *30*, 1321–1327, 1994.

Shaw, B. L., R. A. Pielke, and C. L. Ziegler, A three-dimensional numerical simulation of a great plains dryline, *Mon. Weather Rev.*, *125*, 1489–1506, 1997.

Ulaby, F. T., and E. A. Wilson, Microwave attenuation properties of vegetation canopies, *IEEE Trans. Geosci. Remote Sensing*, *23*, 746–753, 1985.

Viterbo, P., and A. K. Betts, Impact of the ECMWF reanalysis soil water on forecasts of the July 1993 Mississippi flood, *J. Geophys. Res.*, *104*(D16), 19,361–19,366, 1999.

Weitz, A. M., M. Keller, E. Linder, and P. M. Crill, Spatial and temporal variability of nitrogen oxide and methane fluxes from a fertilized tree plantation in Costa Rica, *J. Geophys. Res.*, *104*(D23), 30,097–30,107, 1999.

Wetzel, P. J., and J. T. Chang, Evapotranspiration from nonuniform surfaces—A 1st approach for short-term numerical weather prediction, *Mon. Weather Rev.*, *116*, 600–621, 1988.

Yoo, C., J. B. Valdes, and G. R. North, Evaluation of the impact of rainfall on soil moisture variability, *Adv. Water Resour.*, *21*, 375–384, 1998.

Zhang, D., and R. A. Anthes, A high-resolution model of the planetary boundary layer-sensitivity tests and comparisons with SESAME-79 data, *J. Appl. Meteorol.*, *21*, 1594–1609, 1982.

F. Pan and M. J. Sale, Environmental Sciences Division, Oak Ridge National Laboratory, MS 6335, Oak Ridge, TN 37831-6335, USA. (panf@ornl.gov)

C. D. Peters-Lidard, Hydrological Sciences Branch, Code 974, NASA Goddard Space Flight Center, Greenbelt, MD 20071, USA.

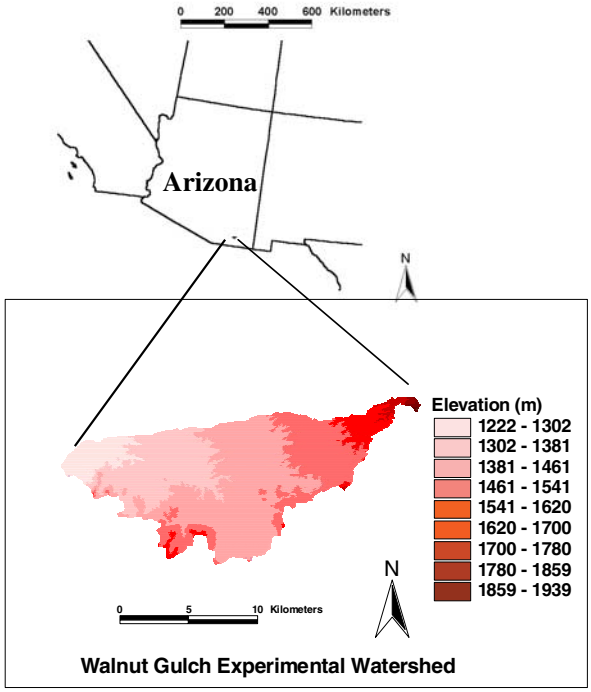

(a) Monsoon'90

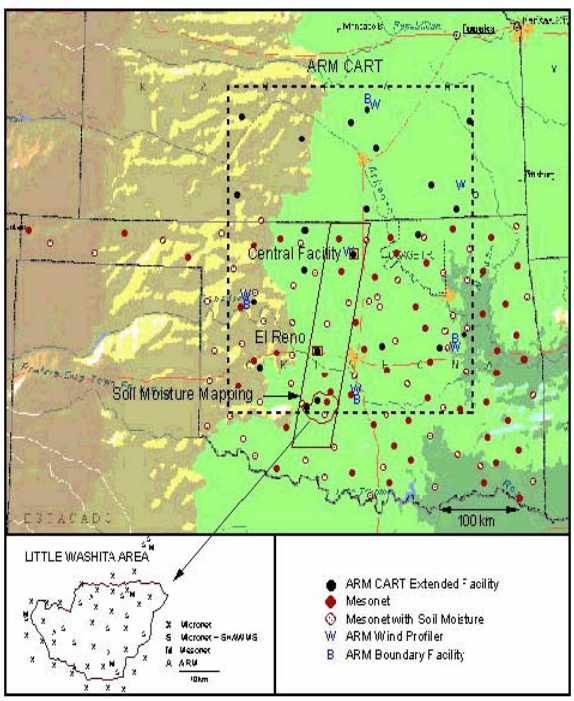

(b) Washita'92 and SGP'97

Figure 2. Location of campaigns studied: (a) Monsoon'90 field experimental domain; (b) SGP'97 field experimental domain. The Little Washita Watershed is inside SGP'97 domain.

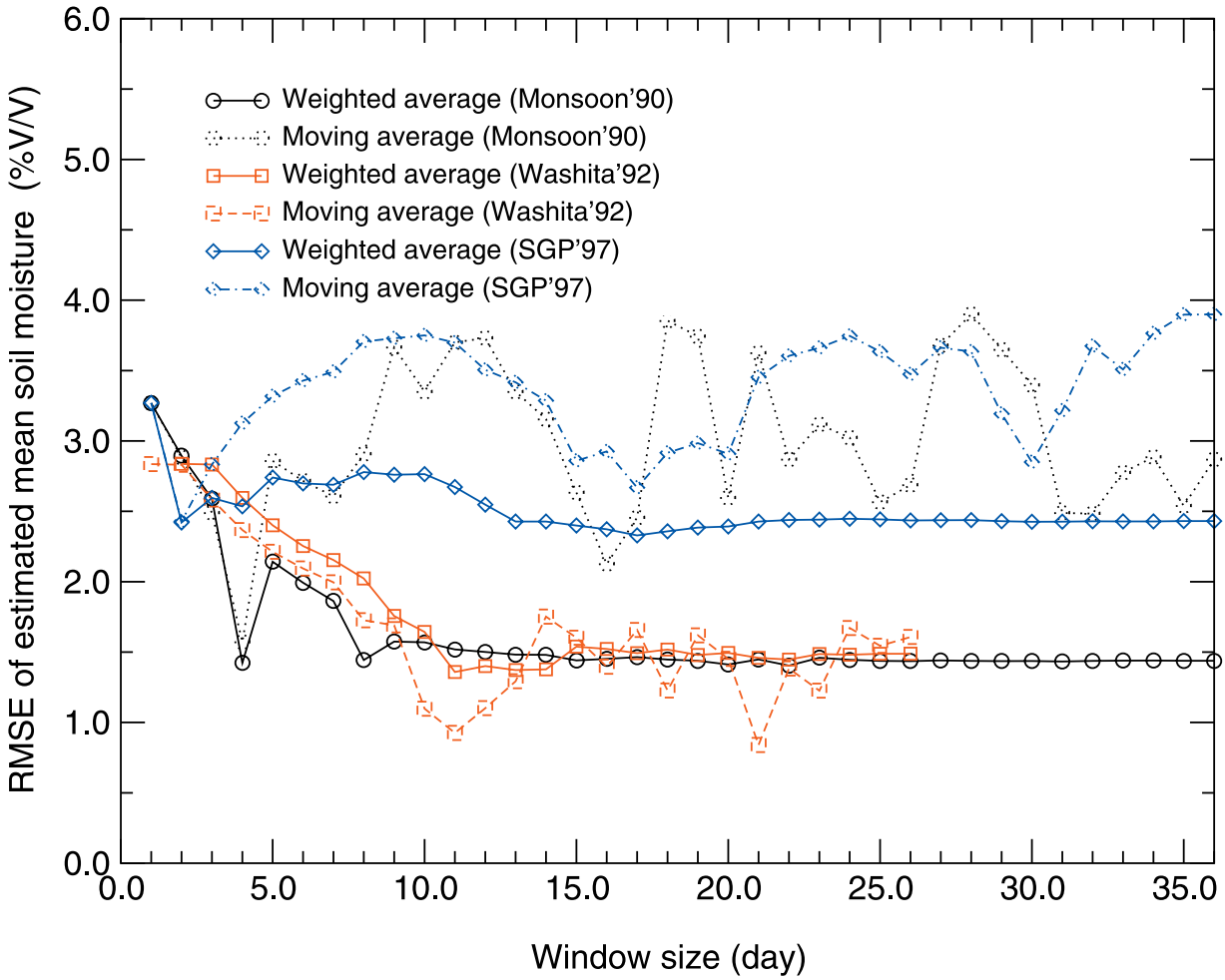

Figure 5. Plot of root mean squared error (RMSE) of the estimated mean soil moisture from rainfall observations versus window size. The loss coefficient is 3.5 m/year for the time-weighted averaging.

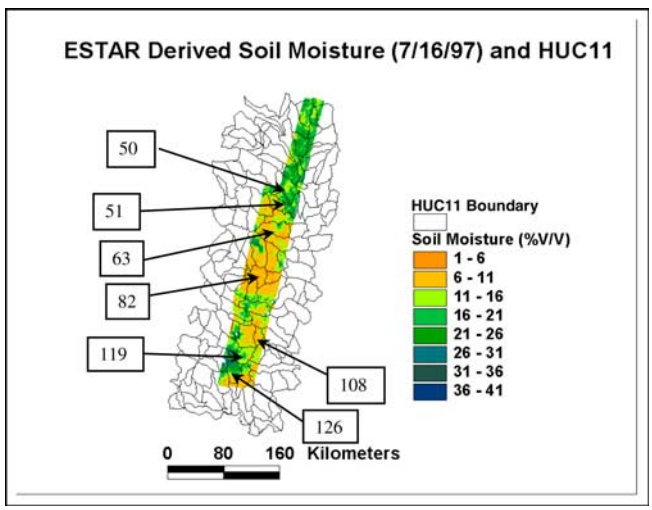

Figure 6. Seven catchments inside SGP'97 domain are used for linking mean soil moisture to mean B values. Map of USGS hydrologic unit code (HUC) with 11 digits is overlapped by Electrically Scanned Thinned Array Radiometer (ESTAR)-derived soil moisture on 7/16/1997 (16 July 1997). The numbers inside the boxes are indices of seven catchments.

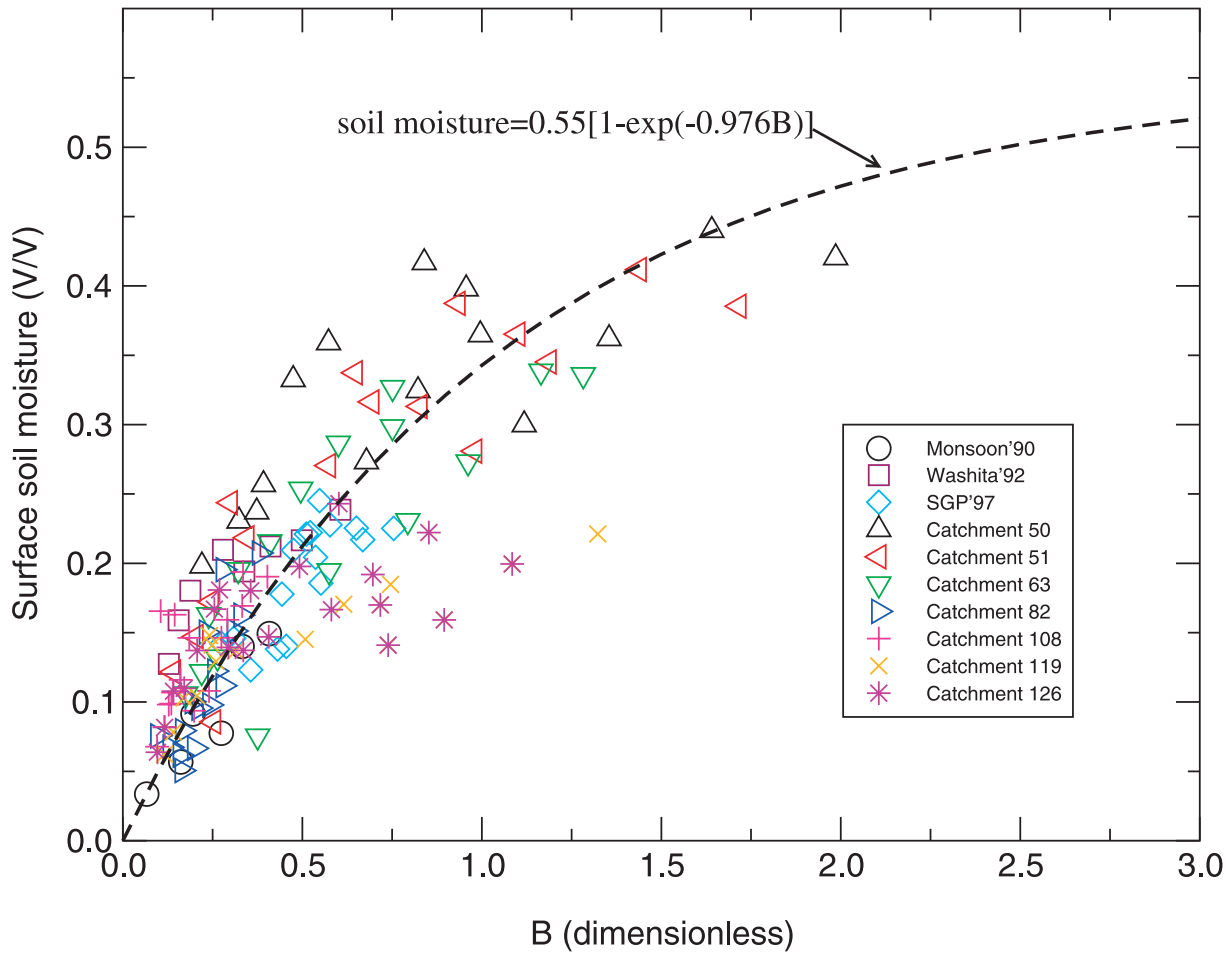

Figure 7. Relation between observed mean soil moisture and mean B values over the Monsoon'90, Washita'92, SGP'97 domains, and seven catchments inside the SGP'97 domain. The dashed line is the empirical relationship between soil moisture and B value.

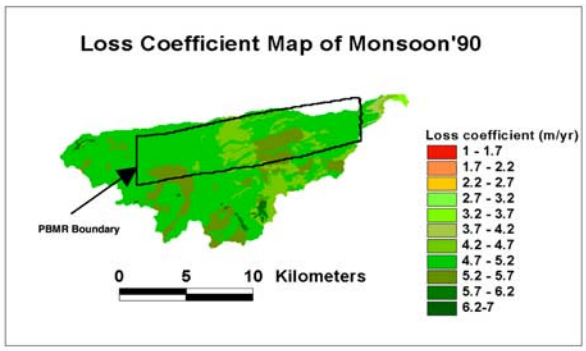

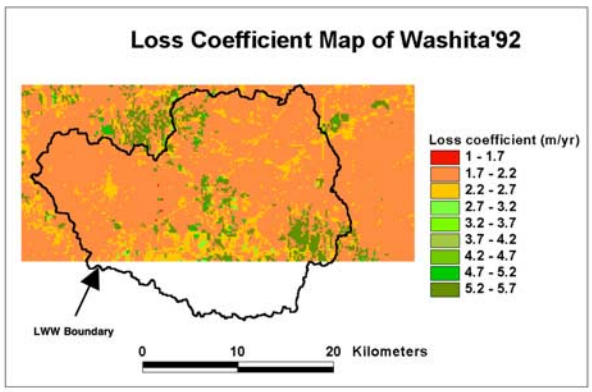

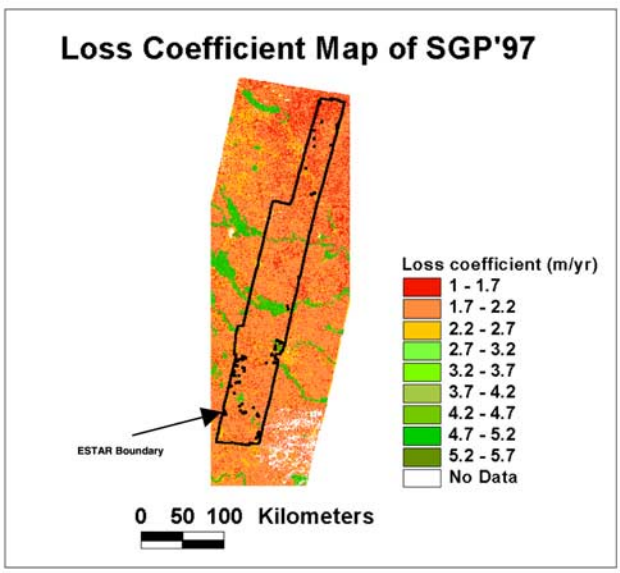

Figure 10. Loss coefficient maps of Monsoon'90, Washita'92, and SGP'97 estimated by equation (15). (PBMR stands for Push Broom Microwave Radiometer and LWW stands for Little Washita Watershed).

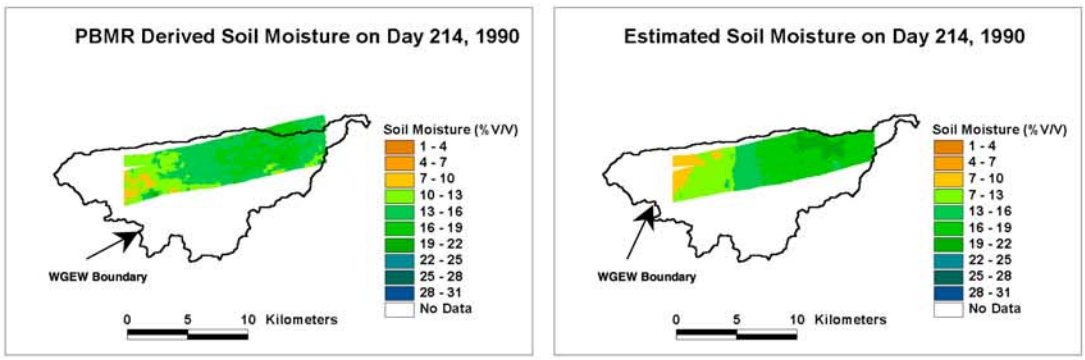

(a) Monsoon'90

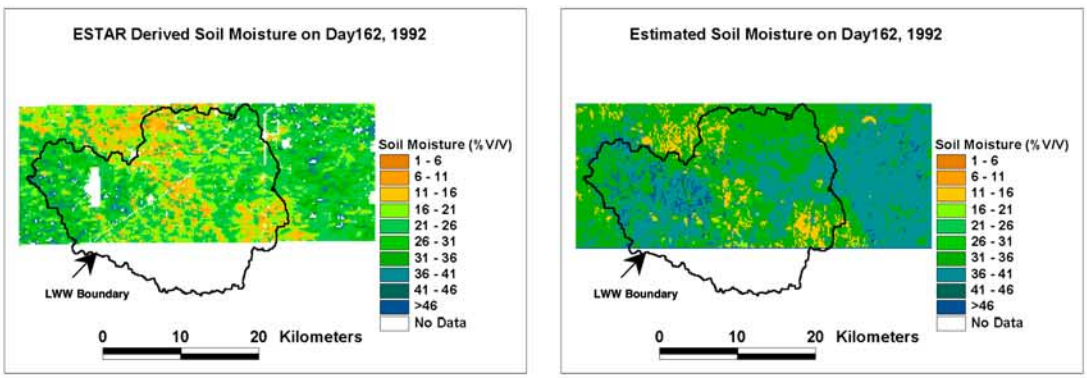

(b) Washita'92

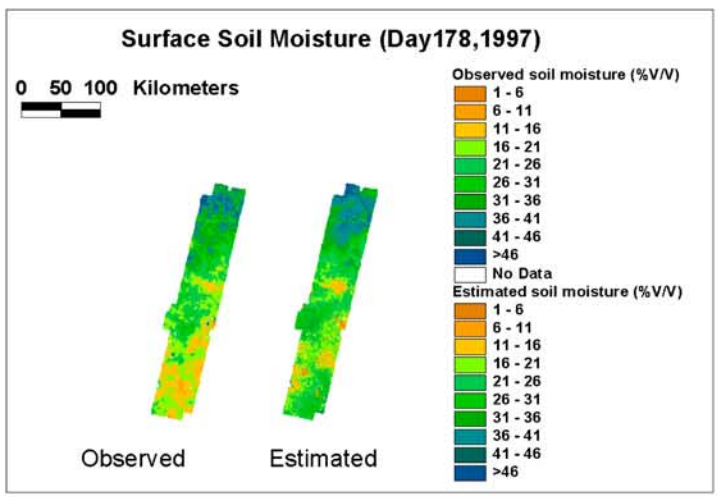

(c) SGP'97

Figure 11. (a) PBMR-derived and estimated soil moisture on day 214 during Monsoon'90; (b) ESTAR-derived and estimated soil moisture on day 162 during Washita'92; (c) ESTAR-derived and estimated soil moisture on day 178 during SGP'97.